Int. J. Solids Structures Vol. 20, No. 5, pp. 455–466, 1984
Printed in Great Britain.

0020–7683/84 $3.00 + .00
Pergamon Press Ltd.

ON THE MECHANICS OF DELAMINATION AND SPALLING IN COMPRESSED FILMS

A. G. EVANS
Materials and Molecular Research Division, Lawrence Berkeley Laboratory, and Department of Materials Science and Mineral Engineering, University of California, Berkeley, CA94720, U.S.A.

and

J. W. HUTCHINSON
Division of Applied Sciences, Harvard University, Cambridge, MA 02138, U.S.A.

(*Received* 8 *March* 1983; *in revised form* 18 *July* 1983)

Abstract—The mechanics of the delamination and spalling of compressed films or coatings has been analyzed using a combination of fracture mechanics and post-buckling theory. It is demonstrated that the delamination of pre-compressed films only occurs if the film buckles, whereupon a stress intensification develops at the buckle perimeter. The associated stress intensity depends on the magnitude of the prestress and the film thickness. Conversely, the delamination of indented coatings occurs without buckling and the stress intensity in this instance depends on the indentation volume, the film thickness and the radius of the delamination. Preliminary attempts have also been made to predict critical spall conditions, following the incidence of buckling.

1. INTRODUCTION

Surface layers subject to substantial residual compression exist in many technological situations. Specifically, films and coatings formed by vapor deposition, sputtering, etc. often develop residual stress during the deposition process itself[1–4]. Additional residual stress may be induced during cooling, when a thermal expansion mismatch exists between the film and the substrate[5, 6]. Oxidation layers formed by inward diffusion of oxygen (e.g. Al_2O_3 on Ni–Cr–Al alloys) also exhibit compression[7, 8], and processes such as machining[9], wear[10] and shot peening generate a residually stressed plastic deformation layer.

Thin layers containing such large residual compressions are susceptible to delamination[11] and spalling[12, 13]. An example[14] is depicted in Fig. 1(a). The initial delamination process occurs by crack extension along a plane parallel to the surface, generally at the film/substrate interface (Fig. 1). Spalling involves the subsequent propagation of the crack through the film. Usually, the crack extension proceeds by brittle rupture mechanisms[14]†. The spalling should thus be characterized by comparative values of the brittle fracture resistance of the interface and the residual crack driving force. Some fundamental features of the crack driving force, pertinent to both delamination and spalling, are considered in the present paper, based on film buckling concepts. Related work has been published[15, 16] on delamination buckling in composite laminated plates, also with emphasis on the interaction between the crack driving force and the buckling behavior of the delaminated region. In fact, one particular result presented within duplicates an earlier result[15].

A similar interface cracking phenomenon accompanies localized plastic indentation of coatings[14] (Fig. 1b). The cracking, in this instance, is associated with the residual compression induced by plastic penetration of the indenter. The interface crack extension induced by controlled indentation of the coating (e. g. using a Vicker's indenter) has been proposed as a simple test for evaluating the adherence of thin coatings[17, 18]. However, quantification of the test requires that an expression for the crack driving force be derived in terms of the identation volume and the film thickness, hardness and modulus. A crack

†Ductile growth may be involved in the delamination that accompanies the wear process in metals[10].

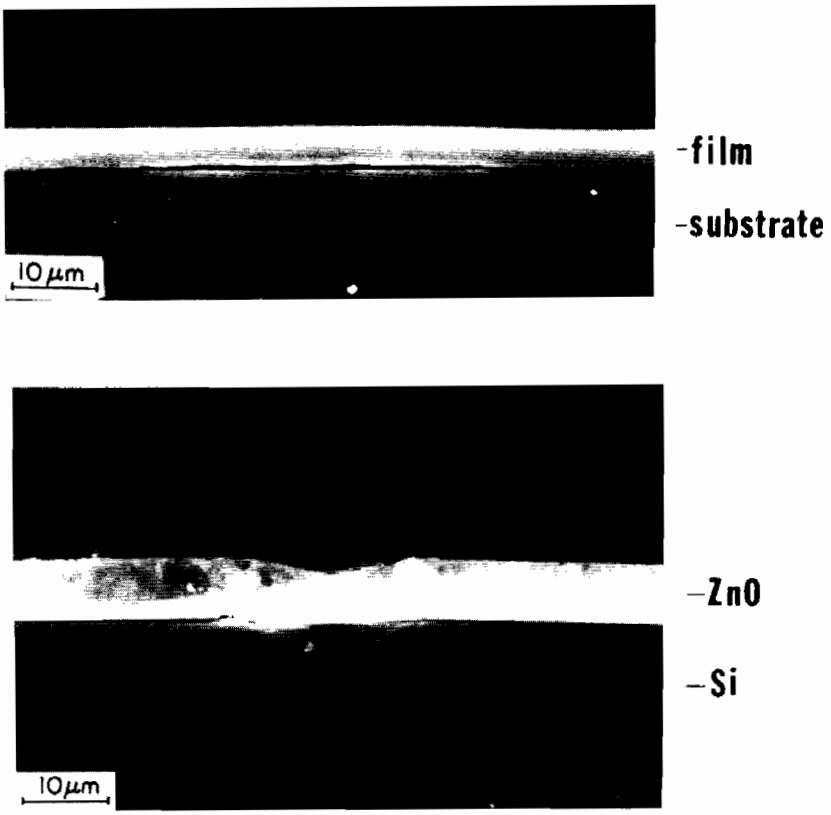

Fig. 1. Scanning electron micrographs of delaminated layers of ZnO on Si: (a) A buckled as-deposited thin film, (b) interface cracking and separation of a thin film induced by indentation.

driving force expression pertinent to this problem is also developed in the present paper and evaluated elsewhere [14].

The buckling problem pertinent to the present set of applications concerns a single interface crack, parallel to the free surface, of sufficient size that the material above the crack can buckle. An alternative buckling situation [19], germane to other applications, envisions many small cracks parallel to the free surface, which lower the overall stress needed to induce a surface buckling mode.

2. THE ENERGY RELEASE RATE FOR DELAMINATION

2.1 *Uniformly compressed film*

In the presence of a small separation (or crack) at the interface between a substrate and a precompressed thin film, the film is susceptible to bucklng, as seen in Fig. 1(a). An interface crack parallel to the free surface (Fig. 2a) clearly does not disturb a stress field, which itself acts parallel to the surface. Hence, a stress concentration at the edge of the crack is not induced. However, if the film buckles away from the substrate (Fig. 2b) the resulting separation generates large tensile stresses at the perimeter of the interface crack, which may induce crack extension. The energy release rate associated with the advance of a crack across a buckled delaminated area can be evaluated by combining results from elastic fracture mechanics and the post-buckling theory of plates.

The first configuration considered is a circular delamination of radius a, as depicted in Fig. 3. A biaxial compression σ_0 is assumed to exist in the film prior to buckling. Interface delamination in the absence of buckling does not cause redistribution of stress or energy release. However, when the delaminated region buckles away from the substrate, there is a release in energy with crack advance which can be determined from the difference, δU, between the elastic strain energy stored in the buckled and unbuckled configurations.

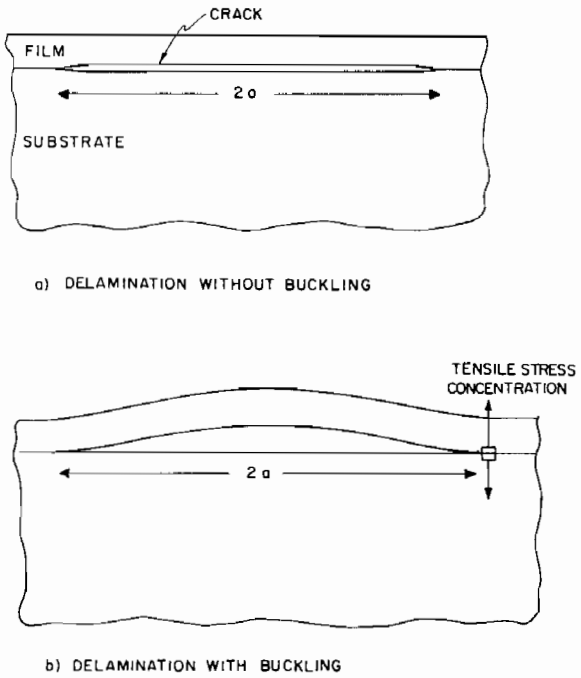

Fig. 2. A schematic showing (a) an interface crack without film buckling and (b) the tensile stress concentration that accompanies film buckling.

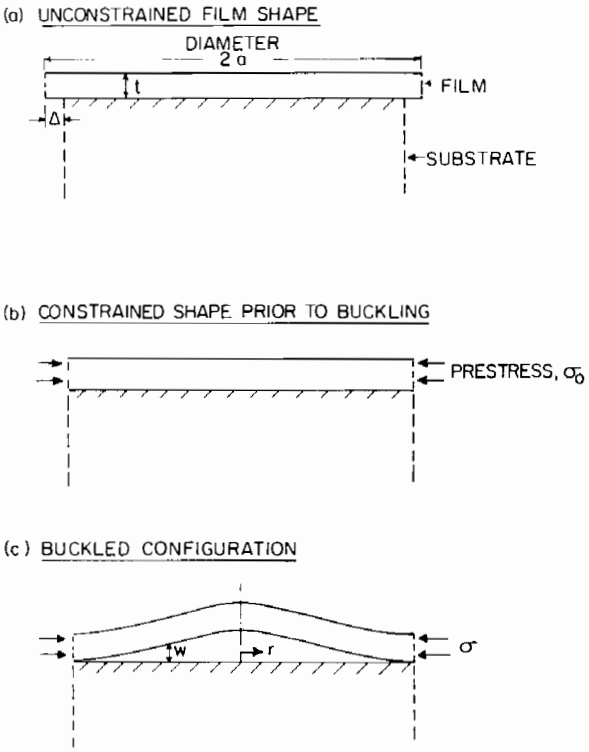

Fig. 3. A schematic illustrating the source of the prestress, σ_0, and the resultant stress, σ, in the buckled configuration.

Specifically, since the change in the energy difference with crack length is equivalent to the total energy release during crack growth, the energy release rate (per unit length of crack edge) attributed to the buckled, delaminated film is[20];

$$\mathscr{G} = (1/2\pi a)(\mathrm{d}\delta U/\mathrm{d}a). \tag{1}$$

The energy difference δU can be estimated by modeling the delaminated region as a clamped circular plate of radius a, as indicated in Fig. 3. This representation is valid if the crack radius, a, is large compared with the film thickness t. Furthermore, by dimensional considerations, it is possible to show that the strain energy change in the substrate, as a result of the stress redistribution due to buckling, is on the order of $a[(\sigma_0 - \sigma)t]^2/E$, while the energy change in the buckled plate is on the order of $a(\sigma_0 - \sigma)^2 at/E$. Thus contribution of the substrate to the strain energy change is on the order of t/a times that from the buckled portion of the film, and it will be neglected. Similarly, the radial deflection of the substrate, where it joins the buckled film at $r = a$, is of the order t/a times the misfit, δa, of the film, given below. Thus, the deflection of the substrate due to buckling of the film will also be neglected.

To carry out the calculation for δU, imagine, as in Fig. 3, that the delaminated region has been separated from its surroundings. In this process, the radius expands due to relief of the biaxial compression, σ_0, by

$$\delta a = (1 - \nu)\sigma_0 a/E \tag{2}$$

where ν is Poisson's ratio and E is Young's modulus. The elastic energy stored in the buckled plate is then equal to the work done by the edge load to force the plate back to an edge radius, a, by assuming that its edge is constrained against rotation. Denoting the compressive edge stress (averaged through the thickness) by σ, so that the edge load (force/unit length) is σt, the plate will undergo buckling if σ exceeds the critical buckling stress for a clamped circular plate[21]

$$\sigma_c = [kE/(12(1 - \nu^2))](t/a)^2 \tag{3}$$

where $k = 14.68$. The associated critical inward radial displacement is

$$\Delta_c = [k/(12(1 + \nu))]t^2/a. \tag{4}$$

A plot of relative edge stress σ/σ_c against the relative inward radial displacement of the edge Δ/Δ_c is shown in Fig. 4. In this plot, the unbuckled branch of the solution has a slope of unity, while the initial slope (at $\sigma = \sigma_c$) of the post-buckled branch is

$$\alpha = (1 + 1.207(1 + \nu))^{-1} \tag{5}$$

($\alpha = 0.383$ for $\nu = 1/3$). This reduction in slope is typical of plate buckling problems. The initial post-buckling slope for a clamped circular plate does not appear to have been previously published. It has been obtained by a slight extension of the calculation by Thompson and Hunt[22]. The full post-buckling response is not available. Nevertheless, experience with other plate buckling problems suggests that the slope does not depart significantly from its initial value, α, until substantial buckling deflections (on the order of several plate thicknesses) are attained. For present purposes the post-buckling response in Fig. 4 will be regarded as linear, with slope α.

The strain energy difference between the unbuckled and buckled states can now be obtained from the area difference between the two load-defection curves (the shaded area in Fig. 4). Specifically, by requiring that $\Delta = \delta a$ and using the critical stress in eqn (3), the total energy difference (when $\sigma_0 > \sigma_c$) becomes

$$\delta U = \pi(1 - \nu)(1 - \alpha)ta^2(\sigma_0 - \sigma_c)^2/E. \tag{6}$$

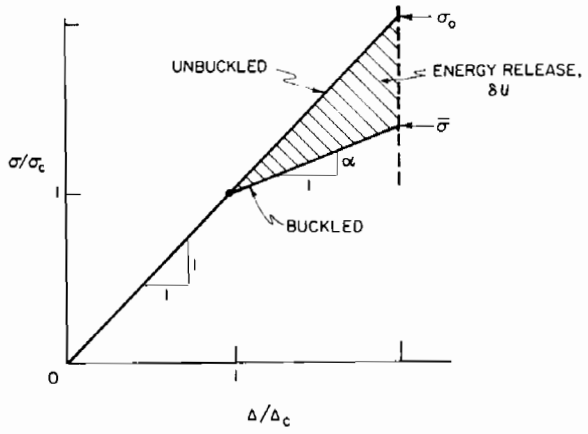

Fig. 4. A plot of the relative edge stress as a function of displacement, for a clamped circular plate, showing the energy release, δU, that accompanies buckling.

The energy release rate deduced from eqns (1) and (6) is thus

$$\mathcal{G} = (1 - \nu)(1 - \alpha)t(\sigma_0^2 - \sigma_c^2)/E. \tag{7}$$

When the elastic properties of the layer and the substrate are different, the singular stress field at the crack tip is more complex than the standard $r^{-1/2}$ field associated with isotropic, homogeneous materials. In the following, for simplicity, any effects stemming from large moduli differences between layer and substrate are ignored so that standard stress intensity factors can be used. (Of course, much of our discussion could equally well be predicated on $\mathcal{G}$.) Conditions at the interface crack involve a combination of opening (Mode I) and shearing (Mode II). Consequently, with the premise that the elastic properties of the system permit the use of a stress intensity factor, K, an effective value may be defined as

$$K^2 = K_I^2 + K_{II}^2 = E\mathcal{G}/(1 - \nu^2), \tag{8}$$

and hence, eqn (7) can be re-expressed as,

$$K/(\sigma_0\sqrt{t}) = [(1 - \alpha)/(1 + \nu)]^{1/2}[1 - (\sigma_c/\sigma_0)^2]^{1/2}. \tag{9}$$

As seen in Fig. 5, when the residual stress $\sigma_0 \gtrsim 3\sigma_c$, K is closely approximated by the asymptote

$$\hat{K}/(\sigma_0\sqrt{t}) = [(1 - \alpha)/(1 + \nu)]^{1/2}. \tag{10}$$

Some related results for the case where the substrate is thin, with application to the delamination buckling of composite plates, have been reported previously[16].

An analogous result can be derived for a two-dimensional buckled region of film, which has a width $2a$ in one direction and is infinite in extent in the other. If σ_0 is now the uniaxial compressive prestress acting perpendicular to the long direction, the effective stress intensity factor is found to be

$$K/(\sigma_0\sqrt{t}) = [2(1 - \nu^2)]^{-1/2}[(1 - \sigma_c/\sigma_0)(1 + 3\sigma_c/\sigma_0)]^{1/2} \tag{11}$$

where now the critical stress is

$$\sigma_c = [\pi^2 E/(12(1 - \nu^2))](t/a)^2. \tag{12}$$

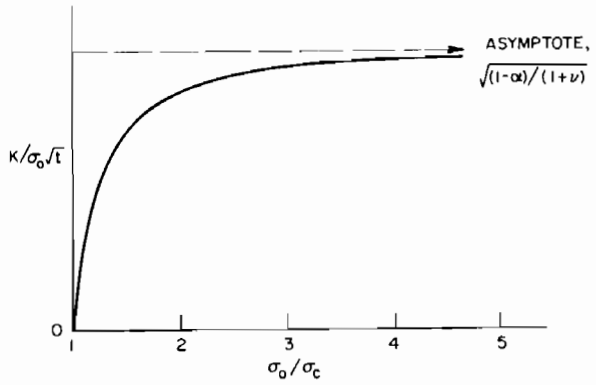

Fig. 5. The variation in stress intensity factor with prestress for a buckled precompressed film.

In this case, the initial post-buckling slope α is that of a wide column, which is very small, $\sim t/a$. It has been taken to be zero in the derivation of eqn (11). In slightly different form, eqn (11) coincides with an earlier result, derived for laminates[15].

2.2 *Indentation induced compression*

Indentations in the surface of brittle solids invariably induce residual stresses[17]. Additionally, in the absence of plastic pile-up, a condition that obtains for most brittle materials,[23–25], and when the indentation induced plastic deformation is confined to the film, the film can be considered subject to dilatation dictated by the indentation volume, V_0. Consequently, when the interface contains a crack of radius, a, and the film is regarded as a clamped circular plate as modeled in Fig. 6(a), the displacement, Δ, that must be imposed at the plate edge to "offset" the dilatation, is given by

$$\Delta \cong V_0/(2\pi at). \tag{13}$$

The corresponding biaxial compressive stress induced in the unbuckled configuration is thus

$$\sigma_0 \equiv E\Delta/[(1-\nu)a] = EV_0/[2\pi(1-\nu)ta^2]. \tag{14}$$

It has again been assumed that $a \gg t$, since the complicated stress distribution within a radius of several thicknesses from the indentation has been ignored. The indentation

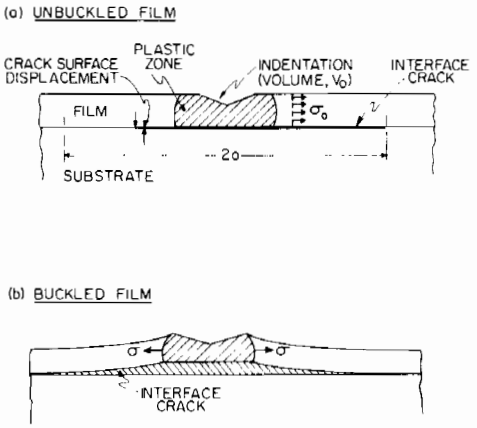

Fig. 6. A schematic showing the stress development attributed to indentation of a thin film, followed by interface fracture.

induced stress σ_0 then depends on the radius, a, of the interface crack, even in the absence of buckling. Consequently, by invoking the critical buckling stress given by eqn (3), the buckling condition can be specified in terms of a critical indentation volume,

$$V_0^c = \pi k t^3/[6(1+\nu)]. \tag{15}$$

If, in the presence of a crack, the strain energy induced by indentation is assumed to reside exclusively in the region above the crack, the strain energy in the unbuckled plate is given by

$$U = \pi a t \sigma_0 \Delta \tag{16}$$

and thus the energy release rate for crack advance is

$$\mathcal{G} \equiv -\frac{1}{2\pi a}\left(\frac{\partial U}{\partial a}\right)_{V_0} = EV_0^2/4\pi^2(1-\nu)a^4 t. \tag{17}$$

The near tip behavior of the unbuckled film should be predominantly Mode II so that $\mathcal{G} \cong (1-\nu^2)\bar{K}_{II}^2/E$, or

$$\bar{K}_{II} = \frac{V_0 E}{2\pi\sqrt{1+\nu}(1-\nu)a^2\sqrt{t}} = \sigma_0\sqrt{t}/\sqrt{1+\nu}. \tag{18}$$

The incidence of buckling for $V_0 > V_0^c$, *reduces* the stored strain energy (Fig. 7) to

$$U = \pi a t \sigma_0 \Delta[1-(1-\alpha)(1-V_0^c/V_0)^2] \tag{19}$$

and, hence, the total effective stress intensity factor, $K^2 = K_I^2 + K_{II}^2$, becomes

$$K = \frac{V_0 E}{2\pi\sqrt{1+\nu}(1-\nu)a^2\sqrt{t}}[1-(1-\alpha)(1-V_0^c/V_0)^2]^{1/2}. \tag{20}$$

Comparison with eqn (18) indicates that buckling reduces the stress-intensity at the crack tip (for corresponding crack radii and when $V_0 \gg V_0^c$) to an amount,

$$K \cong \sqrt{\alpha}\bar{K}_{II}. \tag{21}$$

Furthermore, estimation of the components K_I and K_{II} in the buckled state (Appendix)

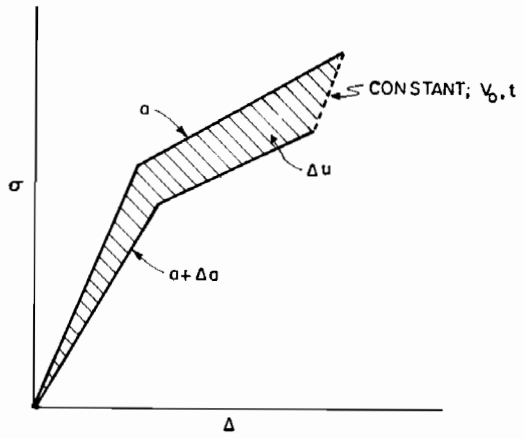

Fig. 7. A schematic illustrating the reduction in strain energy that accompanies crack advance Δa in a buckled, indented thin film.

indicates that for $V_0 \gg V_0^c$,

$$K_I/K_{II} \cong \sqrt{(1-\alpha)/\alpha}. \tag{22}$$

Observations[14] indicate that contact between the film and substrate is often retained immediately beneath the indentation. The existence of a centrally located contact restricts the buckling, otherwise the model of Fig. 3 is applicable. The critical buckling stress associated with the axisymmetric mode of a clamped circular plate constrained to have zero deflection at its center is still given by eqn (3) but now, $k = 42.67$.† The post-buckling slope α has not been determined for this case, but it is expected to be similar to that for the unconstrained circular plate.

3. SPALLING

The approach to spalling of a buckled region, presented within, is intended to provide insight into the parametric dependence of the process. The application of detailed crack branching analyses is not considered. Some related results[26], with primary application to spalling and rocks, illustrate the behavior of cracks under compressive loading when the cracks are not quite parallel to the free surface.

The incidence of spalling requires that the delamination crack deflect upward toward the coating. The stresses at the tip of the delamination should encourage such deflections after buckling has initiated. The details of the crack tip stress field needed to predict the spalling trajectory have not been calculated, but some important insights into the incidence of spalling can be derived by, again, regarding the buckled region as a clamped circular plate. In the following, the component of strain in the radial direction ϵ_r at the bottom edge of the buckled plate is calculated. This component exhibits the largest tension in the buckled configuration and is expected to precipitate the spall.

The vertical deflection of the buckled plate is given by[22],

$$w = \hat{w}[0.287 + 0.713\ J_0(3.83r/a)] \tag{23}$$

where $\hat{w}$ is the deflection at the center, r is the distance from the center of the buckle, and J_0 is the Bessel function of the first kind, of order zero. Post-buckling theory provides the relation between the average edge stress σ and the deflection at the center as[22]

$$\sigma/\sigma_c = 1 + b(\hat{w}/t)^2 \tag{24}$$

where terms of order $(w/t)^4$ have been neglected and $b = 0.205$. In the buckled state

$$\sigma/\sigma_c - 1 = \alpha(\sigma_0/\sigma_c - 1) \tag{25}$$

where α is given by eqn (5). Thus,

$$\hat{w}/t = [(\alpha/b)(\sigma_0/\sigma_c - 1)]^{1/2} \tag{26}$$

The radial strain due to bending at the bottom periphery of the plate ($r = a$) is given by

$$\epsilon_r^b \equiv (t/2)(d^2w/dr^2) = 2.10\hat{w}t/a^2 \tag{27}$$

when $\nu = 1/3$. Combining eqns (26) and (27) gives

$$\epsilon_r^b = 2.87(t/a)^2 \quad (\sigma_0/\sigma_c - 1)^{1/2} \tag{28a}$$

or, by combining with eqn (3), with $k = 14.68$

$$\epsilon_r^b = 2.09(\sigma_c/E)(\sigma_0/\sigma_c - 1)^{1/2}. \tag{28b}$$

†This result for k has been obtained by the authors using an exact analysis of the buckling problem. We have been unable to locate this solution in the standard literature.

Superimposed on the bending strains are the strains due to middle surface stretching. The circumferential stretching strain at the periphery is, $\epsilon_\theta^s = -\sigma_0(1-\nu)/E$, while the radial stress, $\sigma_r = -\sigma$. These two results can be used to determine the radial component of the middle surface stretching strain,

$$\epsilon_r^s = -\sigma(1-\nu^2)/E + \nu(1-\nu)\sigma_0/E. \tag{29}$$

The resulting radial strain at the bottom periphery of the plate is

$$\epsilon_r = \epsilon_r^b + \epsilon_r^s. \tag{30}$$

It is recalled from eqn (9) that the effective stress intensity factor increases monotonically to the asymptote, eqn (10), as the delamination radius increases (for a fixed prestress σ_0). At the same time, ϵ_r increases to a peak tensile value and then decreases with further increase in a. Hence, if spalling is to occur, it is most likely at a delamination radius in the vicinity of the peak in ϵ_r. This peak may be obtained by noting that ϵ_r can be expressed entirely in terms of σ_c and σ_0, using the a-dependence of σ_c in eqn (3). Then, it can be readily shown that the peak value of ϵ_r, for fixed σ_0, with $\nu = 1/3$, is given by;

$$\epsilon_r^* = 5.66\sigma_0/E \tag{31a}$$

attained when

$$(a/t)^* = 1.92(E/\sigma_0)^{1/2}. \tag{31b}$$

The magnitudes of this critical aspect ratio for typical residual stress levels (100–500 MPa) are in the range, 20–50. The critical aspect ratio is interpreted as the relative delamination length at which spalling is *most likely* to occur and should thus, represent the characteristic shape of spalled films.

4. COMPARISON WITH EXPERIMENT

Ample reference can be found to the existence of delamination and spalling in precompressed surface films. However, the authors are not aware of systematic studies that explicitly address this important phenomenon. It is hoped that the present analysis will assist in the design of the critical experiments needed to quantify the incidence of both delamination and eventual spalling.

Indentation induced delamination, or lateral cracking, has been subject to preliminary measurements[27] suitable for initial comparison with the present analysis. The comparison is facilitated by re-expressing the indentation volume in terms of the indentation load, P[17],

$$V \sim (P/H)^{3/2}\cot\Psi \tag{32}$$

where H is the hardness and Ψ is the angle of the indenter. Then, noting that cracking occurs at the base of the plastic zone[27] and hence, that

$$t \sim (P/H)^{1/2}(E/H)^{1/2}\cot^{1/3}\Psi \tag{33}$$

the delamination radius can be deduced from eqn (18) as,

$$a = \lambda\frac{P^{5/8}(E/H)^{3/8}\cot^{5/12}\Psi}{K_c^{1/2}H^{1/8}} \tag{34}$$

where λ is a material independent constant and K_c is the fracture toughness of the material. Lateral fracture data obtained for several materials[27] conform closely with eqn (34), as shown in Fig. 8, such that $\lambda = 0.17$.

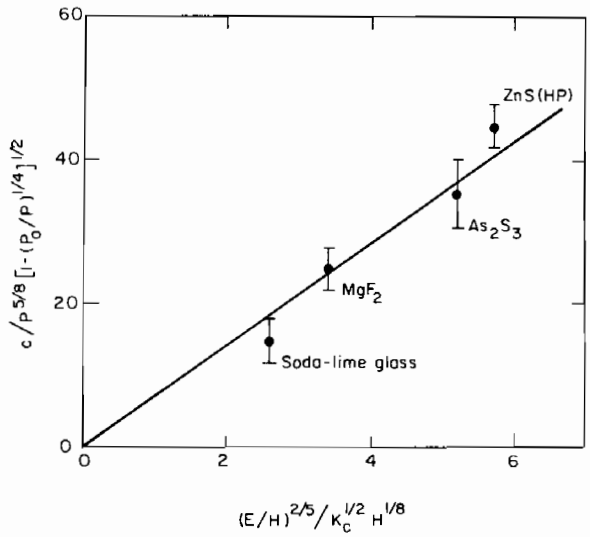

Fig. 8. Lateral fracture data[17] plotted according to the scheme suggested by the buckling analysis, showing conformance with the prediction of this analysis.

5. DISCUSSION

The analysis presented in the preceding sections describes the *growth* phase of the delamination of compressed surface films and their eventual spallation. The process that *initiates* the interface separation has not been given explicit consideration. This deficiency is of least concern for the indentation problem, wherein the crack driving force increases as the delamination radius decreases and hence, initiation occurs quite readily. However, initiation represents a substantial additional issue in uniformly, precompressed films.

Initiation of an interface separation is contingent upon the existence of a normal tensile stress or a shear stress at the interface. Normal tensions and shears do not develop at planar interfaces between precompressed films and their substrates. Hence, the delamination of such interfaces requires a preexistent separation. Contaminated surfaces can, of course, be a source of initial separation when the films are formed by deposition processes. However, the magnitude of the initial separation required to generate a substantial delamination, and subsequent spalling, depends upon the specific origin of the film compression. When the film forms under compression (i.e. during deposition), it is evident from eqn (3) that film buckling initiates immediately ($t \approx 0$) at all initial separations. Then, as the film thickness increases, only the larger initial separations satisfy the buckling requirements. The driving force for delamination at the remaining buckled sections, and its variation with film thickness, can be derived from eqns (9) and (3) as,

$$\frac{K}{\sigma_0\sqrt{t}} = \left[\frac{1-\alpha}{1+\nu}\right]^{1/2}\left[1 - \frac{kE}{12\sigma_0(1-\nu^2)}\left(\frac{t}{a}\right)^2\right]^{1/2}. \tag{35}$$

The trend in driving force, depicted in Fig. 9, indicates the existence of a maximum, $\hat{K}$, given by;

$$\frac{\hat{K}}{\sigma_0\sqrt{a}} = 2\left(\frac{\sigma_0}{kE}\right)^{1/4}\left[\frac{(1-\alpha)(1-\nu)^{1/2}}{3(1+\nu)^{1/2}}\right]^{1/2}. \tag{36}$$

Equating $\hat{K}$ to the critical value for the interface, K_c^i, a critical initial separation radius, a_c, can be derived from eqn (36) as;

$$a_c = \left(\frac{K_c^i}{\sigma_0}\right)^2\left(\frac{kE}{\sigma_0}\right)^{1/2}\left[\frac{3}{4(1-\alpha)}\sqrt{\frac{1+\nu}{1-\nu}}\right] \tag{37}$$

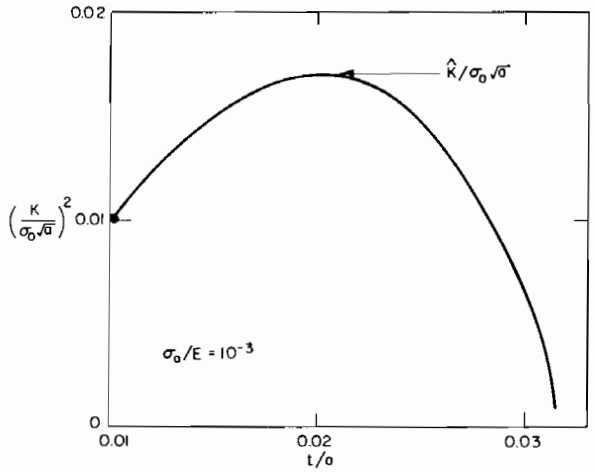

Fig. 9. The variation in stress intensity with film thickness for an initial separation of radius, a.

such that delamination will occur at initial separations with radii $> a_c$. The delamination occurs at a critical film thickness

$$t_c = 2a_c[\sigma_0(1-\nu^2)/kE]^{1/2}. \tag{39}$$

Inserting typical values for the material properties ($\sigma_0 = 3 \times 10^8\ Pa$, $E = 3 \times 10^{11}\ Pa$, $K_c^i = 10^5\ Pa\sqrt{m}$) indicates that $a_c \approx 12\ \mu m$ and $t_c \approx 0.2\ \mu m$. However, it should also be recognized that the specific values of a_c and t_c are very sensitive to variations in the residual stress and the adherence.

The preceding mode of delamination does not pertain to films that generate residual compression during cooling (due to thermal expansion mismatch), nor is it likely to apply to films formed by oxidation, in which the interface translates during film growth and encompasses previously formed separations. In these instances, the initiation of interface separations (in the absence of interface defects of adequate size) requires the existence of normal tensions or shear stresses at the interface. The role of the stresses at such interfaces in the delamination process will be considered in a subsequent publication.

6. CONCLUSION

Analysis of precompressed films has revealed that such films are only susceptible to delamination, and eventual spalling, once film buckling has initiated. A buckling criterion must, therefore, be first satisfied before spallation can occur. After buckling, a stress intensification develops at the perimeter of the delamination. The stress intensity depends on the magnitude of the prestress, σ_0, and the film thickness, t, such that a critical value of the quantity, $\sigma_0\sqrt{t}$, must be exceeded before the delamination can propagate and cause spallation.

The indentation of thin films induces a spatially varying prestress and a stress intensification in the absence of buckling. The stress intensity varies directly with the indentation volume and inversely with the delamination radius and film thickness. In this instance, buckling reduces the stress initiation by about a factor of two. However, eventual spalling is, in all cases, contingent upon buckling and the development of in-plane tensile stress concentration within the film. Preliminary considerations pertinent to spalling conditions, predicated on the magnitude of the buckling stress in the buckled film, indicate that spalling is most likely to occur at a critical value of the ratio of the delamination radius to the film thickness.

Acknowledgements—The authors wish to thank B. Budiansky for helpful insights and input. Funding for this work was provided by the Defense Advanced Research Projects Agency through the University of Michigan and

for one of us (A.G.E.) by the Director, Office of Energy Research, Office of Basic Energy Sciences, Materials Sciences Division of the U.S. Department of Energy under Contract No. DE-AC03-76SF00098, and for the other (J.H.) by the Materials Research Laboratories at Harvard under contract NSF-DMR-80-20247.

REFERENCES

1. W. Kern, G. L. Schable and A. W. Fisher, *RCA Rev.* **37** 3 (1976).
2. A. K. Sinka, H. J. Levistein and T. E. Smith, *J. Appl. Phys.* **49**, 2423 (1978).
3. A. Shintani, S. Sugaki and H. Nakashima, *J. Appl. Phys.* **51**, 4197 (1980).
4. A. Pan and J. E. Green, *Thin Solid Films* **78**, 25 (1981).
5. D. L. Deadmore and C. E. Lowell, *Oxid Met.* **11**, 91 (1977).
6. E. P. Jacobs and G. Dorda, *Surface Sci.* **73**, 357 (1978).
7. J. Stringer, *Corr. Sci.* **10**, 50 (1970).
8. W. Janeckle, S. Leitikow and A. Staedler, *J. Electrochem. Soc.* **111**, 1031 (1964).
9. D. B. Marshall, A. G. Evans, B. T. Khuri-Yakub and G. S. Kino, *Proc. Roy. Soc., London A* **385**, 461 (1983).
10. L. E. Samuels, E. D. Doyle and D. M. Tuley, *Fundamentals of Friction and Wear of Materials* (Edited by D. A. Rigney), p. 13. ASM, Metals Park (1981).
11. N. Matuda, S. Baba and A. Kinbara, *Thin Solid Films* **8**, 301 (1981).
12. R. W. Hoffman, *Physics of Thin Films* (Edited by G. Haas), p. 25. Academic Press, New York. (1981).
13. T. Sumomogi, K. Kuwahara and H. Fujiyama, *Thin Solid Films* **79**, 91 (1981).
14. C. Rossington, D. B. Marshall and A. G. Evans, to be published.
15. H. Chai, C. D. Babcock and W. G. Knauss, One dimensional modelling of failure in laminated plates by delamination buckling. *Int. J. Solids Structures* **17**, 1069–1083 (1981).
16. W. J. Bottega and A. Maewal, Delamination buckling and growth in laminates. *J. Appl. Mech.* **50**, 184–189 (1983).
17. B. R. Lawn, A. G. Evans and D. B. Marshall, *J. Am. Ceram. Soc.* **63**, 574 (1980).
18. S. S. Chiang, D. B. Marshall and A. G. Evans, *Surfaces and Interfaces in Ceramic and Ceramic/Metal Systems* (Edited by J. A. Pask and A. G. Evans), p. 603. Plenum, New York (1981).
19. L. M. Keer, S. Nemat-Nasser and A. Oranratnachai, Surface instability and splitting in compressed brittle elastic solids containing crack arrays, *J. Appl. Mech.* **49**, 761–767 (1982).
20. B. R. Lawn and T. R. Wilshaw, *Fracture of Brittle Solids*. Cambridge University Press (1974).
21. S. Timoshenko and J. M. Gere, *Theory of Elastic Stability*, 2nd Edn. McGraw Hill, New York (1961).
22. J. M. T. Thompson and G. W. Hunt, *A General Theory of Elastic Stability*. Wiley, New York (1973).
23. S. S. Chiang, D. B. Marshall and A. G. Evans, *J. Appl. Phys.* **53**, 298 (1982).
24. T. O. Mulhearn, *J. Mech. Phys. Solids* **7**, 85 (1959).
25. A. G. Atkins and D. Tabor, *J. Mech. Phys. Solids* **13**, 149 (1965).
26. S. Nemat-Nasser and H. Horii, Compression-induced nonplanar crack extension with application to splitting, exfoliation and rockburst. *J. Geophys. Res.* **87**, 6805–6821 (1982).
27. D. B. Marshall, B. R. Lawn and A. G. Evans, *J. Am. Ceram. Soc.* **65**, 561 (1982).

APPENDIX

Estimation of mode I and II stress intensity factors for buckled delamination resulting from indentation

The post-buckling Mode II component of the crack driving force, K_{II}^b, in the indentation problem is given approximately by eqn (18) with the precompression, σ_0, replaced by the edge thrust, (Fig. 3), such that

$$K_{II}^b \approx \sigma\sqrt{t}/\sqrt{1+v}. \tag{A1}$$

Hence, noting eqn (13), and using the same post-buckling relation, as before,

$$\sigma = \sigma_0 - (1-\alpha)\sigma_c[V_0/V_0^c - 1]. \tag{A2}$$

Furthermore, since,

$$\sigma_c/\sigma_0 = V_0^c/V_0 \tag{A3}$$

we obtain,

$$\sqrt{1+v}K_{II}^b/\sigma_0\sqrt{t} = [1 + (1-\alpha)(V_0^c/V_0 - 1)] \tag{A4a}$$

which reduces for $V_0 \gg V_0^c$ to

$$\sqrt{1+v}K_{II}^b/\sigma_0\sqrt{t} = \alpha. \tag{A4b}$$

Now, by combining eqns (8), (20) and (A4a) the Mode I stress intensity factor is

$$\sqrt{1+v}K_I^b/\sigma_0\sqrt{t} = \left\{(1-\alpha)(1 - V_0^c/V_0)[2 - (2-\alpha)(1 - V_0^c/V_0)]\right\}^{1/2} \tag{A5a}$$

which reduces for $V_0 \gg V_0^c$ to,

$$\sqrt{1+v}K_I^b/\sigma_0\sqrt{t} = \sqrt{\alpha(1-\alpha)}. \tag{A5b}$$

The ratio of the stress intensity factor is given by eqn (22) when $V_0 \gg V_0^c$.